Origin of the Fermi Bubble

K.-S. Cheng[1], D. O. Chernyshov[1,2,3], V. A. Dogiel[1,2], C.-M. Ko[3], W.-H. Ip[3]

[1] Department of Physics, University of Hong Kong, Pokfulam Road, Hong Kong, China

[2] I.E.Tamm Theoretical Physics Division of P.N.Lebedev Institute of Physics, Leninskii pr. 53, 119991 Moscow, Russia

[3] Institute of Astronomy, National Central University, Chung-Li 32054, Taiwan

Received _____; accepted _____

ABSTRACT

Fermi has discovered two giant gamma-ray-emitting bubbles that extend nearly 10kpc in diameter north and south of the galactic center (GC). The existence of the bubbles was first evidenced in X-rays detected by ROSAT and later WMAP detected an excess of radio signals at the location of the gamma-ray bubbles. We propose that periodic star capture processes by the galactic supermassive black hole, Sgr A*, with a capture rate $3 \times 10^{-5}\mathrm{yr}^{-1}$ and energy release $\sim 3 \times 10^{52}$erg per capture can produce very hot plasma $\sim$ 10keV with a wind velocity $\sim 10^8$cm/s injected into the halo and heat up the halo gas to $\sim$ 1keV, which produces thermal X-rays. The periodic injection of hot plasma can produce shocks in the halo and accelerate electrons to $\sim$TeV, which produce radio emission via synchrotron radiation, and gamma-rays via inverse Compton scattering with the relic and the galactic soft photons.

Subject headings: Galaxy: halo - galaxies: jets - radiation mechanisms: non-thermal - black hole physics

1. Introduction

Observations reveal many evidences of unusual processes occurring in the region of GC. For instance, the enigmatic 511 keV annihilation emission discovered by INTEGRAL (see e.g. Knoedlseder et al. 2005) whose origin is still debated, the hot plasma with temperature about 10 keV which cannot be confined in the GC and, therefore, sources with a power about 10^{41} erg s^{-1} are required to heat the plasma (Koyama et al. 2007). In fact plasma outflows with the velocity $\gtrsim 100$ km s^{-1} are observed in the nucleus regions of our Galaxy (Crocker et al. 2010a) and Andromeda (Bogdan & Gilfanov 2010). Time variations of the 6.4 keV line and X-ray continuum emission observed in the direction of molecular clouds in the GC which are supposed to be a reflection of a giant X-ray flare occurred several hundred years ago in the GC (Inui et al. 2009; Ponti et al. 2010; Terrier et al. 2010). HESS observations of the GC in the TeV energy range indicated an explosive injection of CR there which might be associated with the supermassive black hole Sgr A*(e.g. Aharonian et al. 2006).

Recent analysis of Fermi LAT data (see Su et al. 2010; Dobler et al. 2010) discovered a new evidence of the GC activity. They found two giant features of gamma-ray emission in the range 1 -100 GeV, extending 50 degrees ($\sim$ 10 kpc) above and below the Galactic center - the Fermi Bubble (FB). They presented a list of mechanisms that may contribute to the energy release and particle production necessary to explain the gamma-ray emission from the bubble. They noticed, however, that most likely the Fermi bubble structure was created by some large episode of energy injection in the GC, such as a past accretion event onto the central supermassive black hole (SMBH) in the last $\sim$ 10 Myr. They cast doubt on the idea that the Fermi bubble was generated by previous starburst activity in the GC because there was no evidence of massive supernova explosions ($\sim 10^4 - 10^5$) in the past $\sim 10^7$ yr towards the GC. Besides, these supernova remnants should be traced by the line

emission of radioactive ^{26}Al. Observations do not show significant concentration of ^{26}Al line towards the GC (Diehl et al. 2006).

Crocker & Aharonian (2010) and Crocker et al. (2010a,b) argued that the procedure used by Su et al. (2010) did not remove contributions of CR interaction with an ionised gas, then gamma-rays could be produced by protons interaction with the fully ionised plasma in the halo. Crocker & Aharonian (2010) also argued that the lifetime of these protons can be very long because the plasma is extremely turbulent in this region therefore protons could be trapped there for a time scale $\tau_{pp} \gtrsim 10^{10}$ yr, then the observed gamma-rays can be explained with the injected power of SN $\sim 10^{39}$ erg s^{-1}.

In this letter we propose that the FB emission may result from star capture processes, which have been developed by Cheng et al. (2006, 2007) and Dogiel et al. (2009a,c,d) to explain a wide range of X-ray and gamma-ray emission phenomena from the GC.

2. Observations

The procedure of separation of the bubble emission from the total diffuse emission of the Galaxy is described in Su et al. (2010). It is important to note that the bubble structure is seen when components of gamma-ray emission produced by cosmic ray (CR) interaction with the background gas, i.e. by CR protons (π^o decay) and electrons (bremsstrahlung) are removed. Su et al. (2010) concluded the the bubble emission was of the inverse Compton (IC) origin generated by relativistic electrons. Here we summarize the multi-wavelength observational constraints of the FB:

- The spectral shape and intensity of gamma-rays are almost constant over the bubble region that suggests a uniform production of gamma-rays in the FB. The total gamma-ray flux from the bubble at energies $E_\gamma > 1$ GeV is $F_\gamma \sim 4 \times 10^{37}$ erg s^{-1}

and the photon spectrum of gamma-rays is power-law, $dN_\gamma/dE_\gamma \propto E_\gamma^{-2}$ for the range 1-100 GeV (Su et al. (2010));

- In the radio range the bubble is seen from the tens GHz WMAP data as a microwave residual spherical excess *("the microwave haze")* above the GC ~ 4 kpc in radius (Finkbeiner 2004). Its power spectrum in the frequency range 23 - 33 GHz is described as power-law, $\Phi_\nu \propto \nu^{-0.5}$. For the magnetic field strength $H \sim 10$ μG the energy range of electrons responsible for emitting these radio waves is within the range 20 - 30 GeV and their spectrum is $dN_e/dE_e \propto E_e^{-2}$;

- The ROSAT 1.5 keV X-ray data clearly showed the characteristic of a bipolar structure (Bland-Hawthorn & Cohen 2003) that aligned well with the edges of the Fermi bubble. The ROSAT structure is explained as due to a fast wind which drove a shock into the halo gas with the velocity $v_{sh} \sim 10^8$cm s^{-1}. This phenomenon requires an energy release of about 10^{55} ergs at the GC and this activity should be periodic on a timescale of $10 - 15$ Myr.

- The similarities of the morphology of the radio, X-ray and gamma-ray structures strongly suggest their common origin.

In the case of electron (leptonic) model of Su et al. (2010) gamma-rays are produced by scattering of relativistic electrons on background soft photons, i.e. relic, IR and optical photons from the disk.

3. The bubble origin in model of a multiple star capture by the central black hole

In this section we present our ideas about the origin of the Fermi Bubble in the framework of star capture by the central SMBH. The process of gamma-ray emission from

the bubble is determined by a number of stages of energy transformation. Each of these stages actually involves complicated physical processes. The exact details of these processes are still not understood very well. Nevertheless, their qualitative features do not depend on these details. In the following, we only briefly describe these processes and give their qualitative interpretations. We begin to describe processes of star capture by the central black hole as presented in Dogiel et al. (2009d).

3.1. Star capture by the central black hole

As observations show, there is a supermassive black hole (Sgr A*) in the center of our Galaxy with a mass of $\sim 4 \times 10^6\ M_\odot$. A total tidal disruption of a star occurs when the penetration parameter $b^{-1} \gg 1$, where b is the ratio of the periapse distance r_p to the tidal radius R_T. The tidal disruption rate ν_s can be approximated to within an order of magnitude $\nu_s \sim 10^{-4} - 10^{-5}$ yr^{-1} (see the review of Alexander 2005).

The energy budget of a tidal disruption event follows from analysis of star matter dynamics. Initially about 50% of the stellar mass becomes tightly bound to the black hole , while the remainder 50% of the stellar mass is forcefully ejected (see, e.g. Ayal et al. 2000). The kinetic energy carried by the ejected debris is a function of the penetration parameter b^{-1} and can significantly exceed that released by a normal supernova ($\sim 10^{51}$ erg) if the orbit is highly penetrating (Alexander 2005),

$$W \sim 4 \times 10^{52} \left(\frac{M_*}{M_\odot}\right)^2 \left(\frac{R_*}{R_\odot}\right)^{-1} \left(\frac{M_{\rm bh}/M_*}{10^6}\right)^{1/3} \left(\frac{b}{0.1}\right)^{-2} \ {\rm erg}\,. \qquad (1)$$

Thus, the mean kinetic energy per escaping nucleon is estimated as $E_{\rm esc} \sim 42 \left(\frac{\eta}{0.5}\right)^{-1} \left(\frac{M_*}{M_\odot}\right) \left(\frac{R_*}{R_\odot}\right)^{-1} \left(\frac{M_{\rm bh}/M_*}{10^6}\right)^{1/3} \left(\frac{b}{0.1}\right)^{-2}$ MeV, where ηM_* is the mass of escaping material. From W and ν_s we obtain that the average power in the form of a flux of subrelativistic protons. If $W \sim 3 \times 10^{52}$ erg and $\nu_s \sim 3 \times 10^{-5}$ yr^{-1}, we get $\dot{W} \sim 3 \times 10^{40}$

erg s^{-1}.

In Dogiel et al. (2009c) we described the injection spectrum of protons generated by processes of star capture as monoenergetic. This is a simplification of the injection process because a stream of charged particles should be influenced by different plasma instabilities,as it was shown by Ginzburg et al. (2004) for the case of relativistic jets. At first the jet material is moved by inertia. Then due to the excitation of plasma instabilties in the flux, the particle distribution functions, which were initially delta functions both in angle and in energy, transforms into complex angular and energy dependencies.

3.2. Plasma heating by subrelativistic protons

Subrelativistic protons lose their energy mainly by Coulomb collisions, i.e. $\frac{dE_p}{dt} = -\frac{4\pi n e^4}{m_e \mathrm{v_p}} \ln\Lambda$, where $\mathrm{v_p}$ is the proton velocity, and $\ln\Lambda$ is the Coulomb logarithm. In this way the protons transfer almost all their energy to the background plasma and heat it. This process was analysed in Dogiel et al. (2009c,d). For the GC parameters the average time of Coulomb losses for several tens MeV protons is several million years. The radius of plasma heated by the protons is estimated from the diffusion equation describing propagation and energy losses of protons in the GC (Dogiel et al. 2009b). This radius is about 100 pc. The temperature of heated plasma is determined by the energy which these protons transfer to the background gas. For $\dot{W} \sim 10^{40} - 10^{41}$erg s^{-1} the plasma temperature is about 10 keV (Koyama et al. 2007) just as observed by Suzaku for the GC. The plasma with such a high temperature cannot be confined at the GC and therefore it expands into the surrounding medium.

3.3. The hydrodynamic expansion stage

Hydrodynamics of gas expansion was described in many monographs and reviews (see e.g. Bisnovatyi-Kogan & Silich 1995). As the time of star capture may be smaller than the time of proton energy losses, we have almost stationary energy release in the central region with a power $\dot{W} \sim 3 \times 10^{40}$ erg s^{-1}. This situation is very similar to that described by Weaver et al. (1977) for a stellar wind expanding into a uniform density medium. The model describes a star at time t=0 begins to blow a spherically symmetric wind with a velocity of stellar wind V_w, mass-loss rate $dM_w/dt = \dot{M}_w$, and a luminosity $L_w = \dot{M}_w V_w^2/2$ which is analogous to the power $\dot{W}$ produced by star capture processes. Most of the time of the evolution is occupied by the so-called snowplow phase when a thin shock front is propagating through the medium . The shock is expanding as

$$R_{sh}(t) = \alpha \left(\frac{L_w t^3}{\rho_0} \right)^{1/5} \tag{2}$$

where $\rho_0 = n_0 m_p$ and α is a constant of order of unity. The velocity distribution inside the expanding region $u(z)$ is nonuniform.

Our extrapolation of this hydrodynamic solution onto the Fermi bubble is, of course, rather rough. First, the gas distribution in the halo is nonuniform. Second, the analysis does not take into account particle acceleration by the shock. A significant fraction of the shock energy is spent on acceleration that modify the shock structure. Nevertheless, this model presents a qualitative picture of a shock in the halo.

3.4. Shock wave acceleration phase and non-thermal emission

The theory of particle acceleration by shock is described in many publications. This theory has been developed, and bulky numerical calculations have beeen performed to calculate spectra of particles accelerated by supernova (SN) shocks and emission produced

by accelerated electrons and protons in the range from radio up to TeV gamma-rays (see e.g. Berezhko & Voelk 2010). Nevertheless many aspects of these processes are still unclear. For instance, the ratio of electrons to protons accelerated by shocks is not reliably estimated (see Bykov & Uvarov 1999).

We notice that the energy of shock front expected in the GC is nearly two orders of magnitude larger than that of the energy released in a SN explosion. Therefore, process of particle acceleration in terms of sizes of envelope, number of accelerated particles, maximum energy of accelerated particles, etc. may differ significantly from those obtained for SNs. Below we present simple estimations of electron acceleration by shocks.

The injection spectrum of electrons accelerated in shocks is power-law, $Q(E_e) \propto E_e^{-2}$, and the maximum energy of accelerated electrons can be estimated from a kinetic equation describing their spectrum at the shock (Berezinskii et al. 1990), $E_{max} \simeq v_{sh}^2/D\beta$, where $v_{sh} \sim 10^8$cm/s is the velocity of shock front, D is the diffusion coefficient at the shock front and the energy losses of electrons (synchrotron and IC) are: $dE_e/dt = -\beta E_e^2$. Recall β is a function of the magnetic and background radiation energy densities, $\beta \sim w\sigma_T c/(m_e c^2)^2$, where σ_T is Thompson cross section and $w = w_{ph} + w_B$ is the combined energy density of background photons w_{ph} and the magnetic energy density w_B respectively. It is difficult to estimate the diffusion coefficient near the shock. For qualitative estimation, we can use the Bohm diffusion ($\sim r_L(E_e)$c), where r_L is the Larmor radius of electrons. Using the typical values of these parameters, we obtain $E_{max} \sim 1\ TeV\ v_8 B_{-5}^{1/2} w_{-12}^{-1/2}$, where v_8 is the shock velocity in units of 10^8cm/s, B_{-5} is the magnetic field in the shock in units of 10^{-5}G and w_{-12} is the energy density in units of 10^{-12}erg/cm^3.

The spectrum of electrons in the bubble is modified by processes of energy losses and escape. It can be derived from the kinetic equation

$$\frac{d}{dE}\left(\frac{dE}{dt}N\right) + \frac{N}{T} = Q(E) \tag{3}$$

where $dE/dt = \beta E^2 + \nabla u(z) E$ describes the inverse Compton, synchrotron and adiabatic (because of wind velocity variations) energy losses, T is the time of particle escape from the bubble, and $Q(E) = KE^{-2}\theta(E_{max} - E)$ describes particles injection spectrum in the bubble. As one can see, in general case the spectrum of electrons in the bubble cannot be described by a single power-law as assumed by Su et al. (2010). The spectrum of electrons has a break at the energy $E_b \sim 1/\beta T$ where T is the characteristic time of either particle escape from the bubble or of the adiabatic losses, e.g. for $\nabla u = \alpha$ the break position follows from $T \sim 1/\alpha$. By solving equation 3, we can see that the electron spectrum cannot be described by a single power-law even in case of power-law injection (see eg. Berezinskii et al., 1990).

The distribution of background photons can be derived from GALPROP program. The average energy density of background photons in the halo are $w_o = 2$ eV cm^{-3} for optical and $w_{IR} = 0.34$ eV cm^{-3} for IR. These background soft photon energy densities are obviously not negligible in comparing with $w_{CMB} = 0.25$ eV cm^{-3} for the relic photons and also comparable with the magnetic energy density ($\sim 1(H/5 \times 10^{-6}G)^2 eV/cm^3$). The expected IC energy flux of gamma-rays and synchrotron radiation emitted from the same population of electrons described above are shown in Fig. 1 for different values of E_b and E_{max}. The Klein-Nishina IC cross-section (Blumenthal & Gould 1970) is used. The observed spectrum of radioemission in the range 5-200GHz and gamma-rays are taken from Dobler & Finkbeiner (2008) and Su et al. (2010) respectively. The inverse Compton gamma ray spectrum is formed by scattering on three different components of the background photons. When these three components are combined (see Fig. 1b), they mimic a photon spectrum E_γ^{-2} and describe well the data shown in Fig. 23 of Su et al. (2010). We want to remark that although a single power law with the spectral indexes in between 1.8 and 2.4 in the energy range of electrons from 0.1 to 1000 GeV can also explain both the Fermi data as well as the radio data as suggested by Su et al. (2010). Theoretically a more complicated

electron spectrum will be developed when the cooling time scale is comparable with the escape time even electrons are injected with a single power law as shown in equation 3.

3.5. The thermal emission from heated plasma

In our model there is 10keV hot plasma with power $\dot{W} \sim 3 \times 10^{40}$erg/s injected into bubbles. Part of these energies are used to accelerate the charged particles in the shock but a good fraction of energy will be used to heat up the gas in the halo due to Coulomb collisions. The temperature of halo gas can be estimate as $nd^3kT \approx \dot{W}d/v_w$ which gives $kT \sim 1.5(\dot{W}/3 \times 10^{40}erg/s)v_8^{-1}(d/5kpc)^{-2}(n/10^{-3})$keV. The thermal radiation power from the heated halo gas is simply given by $L_{th} = 1.4 \times 10^{-27} n_e n_i Z^2 T^{1/2}$erg/cm^3 (Rybicki & Lightman 1979). By using kT=1.5keV, $n_e = n_i = 10^{-3}cm^{-3}$ and Z=1, we find $L_x \sim 10^{38}$erg/s.

4. Discussion

The observed giant structure of FB is difficult to be explained by other processes. We suggest that periodic star capture processes by the central SMBH can inject $\sim 3 \times 10^{40}$erg/s hot plasma into the galactic halo. The hot gas can expand hydrodynamically and form shock to accelerate electrons to relativistic speed. Synchrotron radiation and inverse Compton scattering with the background soft photons produce the observed radio and gamma-rays respectively. Acceleration of protons by the same shock may contribute to Ultra-high energy cosmic rays, which will be considered in future works.

It is interesting to point out that the mean free path of TeV electrons $\lambda \sim \sqrt{D/\beta E_e} \sim 50 D_{28}^{1/2} \tau_5^{1/2}$pc, where D_{28} and τ_5 are the diffusion coefficient and cooling time for TeV electrons in units of $10^{28}cm^2/s$ and 10^5yrs respectively. This estimated mean free path is

much shorter than the size of the bubble. In our model the capture time is once every $\sim 3 \times 10^4$yr, we expect that there is about nearly 100 captures in 3 million years. Each of these captures can produce an individual shock front, therefore the gamma-ray radiation can be emitted uniformly over the entire bubble.

Furthermore we can estimate the shape of the bubble, if we simplify the geometry of our model as follows. After each capture a disk-like hot gas will be ejected from the GC. Since the gas pressure in the halo $(n(r)kT \sim 10^{-14}(n/3 \times 10^{-3}cm^{-3})(T/3 \times 10^4 K)\mathrm{erg/cm^3})$ is low and decreases quadratically for distance larger than 6kpc(Paczynski 1990), we can assume that the hot gas can escape freely vertically, which is defined as the z-direction and hence the z-component of the wind velocity $v_{wz} = constant$ or $z = v_{wz}t$. The ejected disk has a thickness $\Delta z = v_{wz}t_{cap}$, where $t_{cap} = 3 \times 10^4$yr is the capture time scale. On the other hand the hot gas can also expand laterally and its radius along the direction of the galactic disk is given by $x(t) = v_{wx}t + x_0 \approx v_{wx}t$, where $x_0 \sim 100pc$(cf. section 3.2). When the expansion speed is supersonic then shock front can be formed at the edge of the ejected disk. In the vertical co-moving frame of the ejected disk the energy of the disk is ΔE, which is approximately constant if the radiation loss is small. The energy conservation gives $\Delta E = \frac{1}{2}mv_{wx}^2$ with $m = m_0 + m_s(t) = m_0 + \pi x^2 \Delta z \rho$, where $m_0 \approx 2\Delta E/v_w^2$ is the initial mass in the ejected disk, m_s is the swept-up mass from the surrounding gas when the disk is expanding laterally, and $\rho = m_p n$ is the density of the medium surrounding the bubble. Combing the above equations, we can obtain $\Delta E = \frac{1}{2}[m_0 + \pi(v_{wx}t)^2 \Delta z \rho]v_{wx}^2$. There are two characteristic stages, i.e. free expansion stage, in which $v_{wx} \approx$constant for $m_0 > m_s(t)$ and deceleration stage for $m_0 < m_s(t)$. The time scale switching from free expansion to deceleration is given by $m_0 = m_s(t_s)$ or $t_s = \sqrt{m_0/\pi \Delta z \rho v_{wx}^2}$. In the free expansion stage, we obtain $x = \frac{v_{wx}}{v_{wz}}z \sim z$ for $x < v_{wx}t_s = x_s$. In the deceleration stage, $\Delta E \approx \frac{1}{2}\pi(v_{wx}t)^2 \Delta z \rho v_{wx}^2$, we obtain $(x/v_w t_s) = \left(\frac{\Delta E}{\pi t_s^2 v_{wx}^4 \Delta z \rho}\right)^{1/4}\left(\frac{z}{v_w t_s}\right)^{1/2} \approx 0.9\left(\frac{z}{v_w t_s}\right)^{1/2}$, we have approximated $v_{wx} \sim v_{wz} \sim v_w \sim 10^8$cm/s, $\Delta E = 3 \times 10^{52}$ergs and $\rho/m_p = 3 \times 10^{-3}cm^{-3}$. The switching

from a linear relation to the quadratic relation takes place at $z_s \sim v_w t_s \sim 300$pc. The quasi-periodic injection of disks into the halo can form a sharp edge, where shock fronts result from the laterally expanding disks with quadratic shape, i.e. $z \sim x^2$. In fitting the gamma-ray spectrum it gives $E_b \sim 50$GeV, which corresponds to a characteristic time scale of either adiabatic loss or particle escape ~ 15Myrs. By using equation 2, the characteristic radius of FB is about 5kpc, which is quite close to the observed size of FB.

We thank the anonymous referee for very useful suggestions and Y.W. Yu for useful discussion. KSC is supported by a grant under HKU 7011/10p. VAD and DOC are partly supported by the NSC-RFBR Joint Research Project RP09N04 and 09-02-92000-HHC-a. CMK is supported in part by the National Science Council, Taiwan, under grants NSC 98-2923-M-008-001-MY3 and NSC 99-2112-M-008-015-MY3.

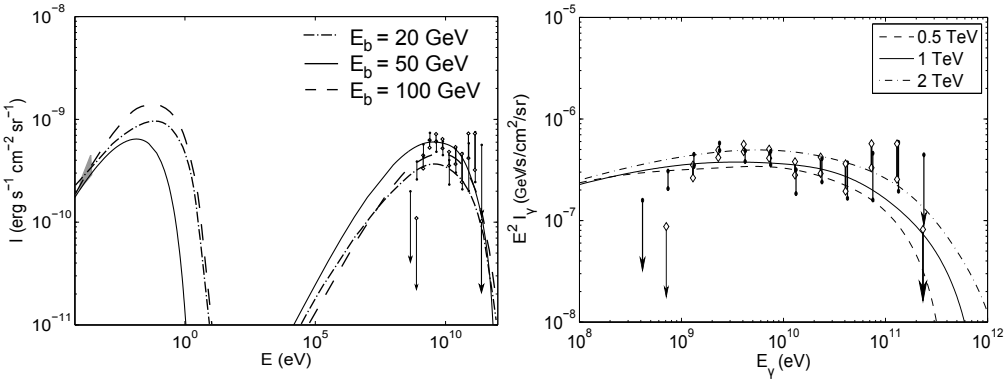

Fig. 1.— (a)Energy fluxes produced by Synchrotron and IC with E_{max}=1TeV and different E_b. (b)The gamma-ray spectra with E_b=50GeV and different E_{max}. .

REFERENCES

Aharonian, F., Akhperjanian, A. G., Bazer-Bachi, A. R. et al. 2006, Nature, 439, 695

Alexander, T. 2005, PhR, 419, 65

Ayal, S., Livio, M., and Piran, T. 2000, ApJ, 545, 772

Berezhko, E. G.; Voelk, H. J. 2010, A&A, 511, 34

Berezinskii, V. S., Bulanov, S. V., Dogiel, V. A., Ginzburg, V. L., and Ptuskin, V. S. 1990, *Astrophysics of Cosmic Rays*, ed. V.L.Ginzburg, (Norht-Holland, Amsterdam)

Bisnovatyi-Kogan, G. S., & Silich, S. A. 1995, RvMP, 67, 661

Blumenthal, G. R., & Gould, R. J. 1970, RvMP, 42, 237

Bogdan, A., & Gilfanov, M. 2010, MNRAS, 405, 209

Bland-Hawthorn, J. & Cohen, M. 2003, ApJ, 582, 246

Bykov, A. M., & Uvarov, Yu. A. 1999, JETP, 88, 465

Cheng, K.-S., Chernyshov, D. O., and Dogiel, V. A. 2006, ApJ, 645, 1138.

Cheng, K.-S., Chernyshov, D. O., and Dogiel, V. A. 2007, A&A, 473, 351.

Crocker, R., & Aharonian, F. 2010, arXiv1008.2658

Crocker, R. M., Jones, D. I., Aharonian, F. et al. 2010a, MNRAS, 411, L11

Crocker, R. M., Jones, D. I., Aharonian, F. et al. 2010b, arXiv1011.0206

Diehl, R., Prantzos, N., & von Ballmoos, P. 2006, Nuclear Physics A, 777, 70

Dobler, G., Finkbeiner, D. P. 2008, ApJ, 680, 1222

Dobler, G. & Finkbeiner, D. P., Cholis, I. et al. 2010, ApJ, 717, 825

Dogiel, V., Cheng, K.-S., Chernyshov D. et al. 2009a, PASJ, 61, 901

Dogiel, V., Chernyshov D., Yuasa, T. et al. 2009b, 61, PASJ, 1093

Dogiel, V., Chernyshov D., Yuasa, T. et al. 2009c, 61, PASJ, 1099

Dogiel, V. A., Tatischeff, V., Cheng, K.-S. et al. 2009d, A&A, 508, 1

Finkbeiner, D. P. 2004, ApJ, 614, 186

Ginzburg, S. L., D'Yachenko, V. F., Paleychik, V. V., Sudarikov, A. L., & Chechetkin, V. M. 2004, Astronomy Letters, 30, 376

Inui, T., Koyama, K., Matsumoto, H., & Tsuru, T.G. 2009, PASJ, 61, S241

Knoedlseder, J., Jean, P., Lonjou, V. et al. 2005, A&A, 441, 513

Koyama, K., Hyodo, Y., Inui, T. et al. 2007, PASJ, 59, 245

Paczynski, B. 1990, ApJ, 348, 485

Ponti, G., Terrier, R., Goldwurm, A. et al. 2010, ApJ, 714, 732

Rybicki, G.B. & Lightman, A.L. 1979, "Radiative Processes in Astrophysics", New York: Wiley

Su, M., Slatyer, T. R., & Finkbeiner, D. P. 2010, ApJ, 724, 1044

Terrier, R., Ponti, G., Belanger, G. et al. 2010, ApJ, 719, 143

Weaver, R., McCray, R., Castor, J., Shapiro, P., and Moore, R. 1977, ApJ, 218, 377